Measurements of the Ice Water Content of Cirrus in the Tropics and Subtropics I: Instrument Details and Validation

E. M. Weinstock, J. B. Smith, D. Sayres, J. V. Pittman, N. Allen, J. Demusz, M. Greenberg, M. Rivero, and J. G. Anderson

Department of Chemistry and Chemical Biology, Harvard University, Cambridge MA 02138

Abstract: We describe an instrument mounted in a pallet on the NASA WB-57 aircraft that is designed to measure the sum of gas phase and solid phase water, or total water, in cirrus clouds. Using an isokinetic inlet, a 600-watt heater mounted directly in the flow, and Lyman-alpha photofragment fluorescence technique for detection, accurate measurements of total water have been made over almost three orders of magnitude. Isokinetic flow is achieved with an actively controlled roots pump by referencing aircraft pressure, temperature, and true air speed, together with instrument flow velocity, temperature, and pressure. During CRYSTAL FACE, the instrument operated at duct temperatures sufficiently warm to completely evaporate particles up to 150μm diameter. In flight diagnostics, intercomparison with water measured by absorption in flight, as well as intercomparisons in clear air with water vapor measured by the Harvard water vapor instrument and the JPL infrared tunable diode laser hygrometer validate the detection sensitivity of the instrument and illustrate minimal hysteresis from instrument surfaces. The simultaneous measurement of total water and water vapor in cirrus clouds yields their ice water content.

Introduction

We describe here a new instrument that combines an isokinetic inlet, a heated duct, and a photofragment fluorescence detection axis for the quantitative measurement of cloud ice water content. It has flown on the NASA WB-57 research aircraft during the Clouds and Water Vapor in the Climate System mission (CWVCS) based out of San Jose, Costa Rica in the summer of 2001 and during the Cirrus Regional Study of Tropical Anvils and Cirrus Layers-Florida Area Cirrus Experiment, known as CRYSTAL FACE (CF), from Key West Florida in July 2002. When combined with simultaneous water vapor measurements, instrument accuracy and response time can be evaluated in clear air, and ice water content can be determined when clouds are sampled. In this manuscript, we illustrate how in-flight diagnostics and intercomparisons with the Harvard water vapor instrument help validate the accuracy of these measurements. We compare results with other total water measurements from the WB-57 during the CF mission and highlight results from flights from both the CWVCS and CF missions.

Accurate measurements of the ice water content (IWC) of cirrus clouds are required for understanding their radiative properties, their impact on the water vapor budget of the upper troposphere and lower stratosphere, and for validation and calibration of satellite-borne instruments that measure cloud properties [Stephens et al., 2002]. The critical need for accurate measurements of cloud ice water content can be succinctly summarized by a statement by the Intergovernmental Panel on Climate Change (IPCC) "As has been the case since the first IPCC report in 1990, probably the greatest uncertainty in future projections of climate arises from clouds and their interactions with radiation." [Houghton et al., 2001]. Toward this end, general circulation models bear the brunt of the prediction responsibility, and the greatest source of uncertainty within these models is the characterization of cirrus clouds. For example, according to the authors of the CF plan, "The ice water content and radiative properties of tropical cirrus systems are so poorly understood that no useful constraints exist for their parameterization in general circulation models (GCMs)."

In previous measurement campaigns, for example the Subsonic Aircraft: Contrail and Cloud Effects Special Study (SUCCESS), Liou et al. [1998] define a mean effective ice crystal radius to determine ice water content from particle measurements. However, this method requires a priori knowledge of the effective density of ice for cloud crystals. This is not only a very elusive parameter, but also one that will vary depending on cloud habit. Bulk ice water content measurements in combination with measurements of particle size and number density have been used to parameterize the effective ice density for a series of in situ cloud encounters. [Heymsfeld et al., 2003a, 2003b]. However, sampling issues exacerbate the difficulty of making accurate in situ measurements of ice particle densities, size distributions, and ice water content. Additionally, the characterization by millimeter wave radar of clouds from ground sites or satellites do not measure ice water content directly, but rather backscattered radiation. The determination of IWC from radar reflectivity requires an assumption of a functional form for the particle size distribution as well as an effective ice density, with its dependence on particle size [Mace et al., 1998].

Calculations of the radiative effects of tropical thin cirrus [e.g. Stackhouse and Stephens, 1991] illustrate potential radiative heating effect of high altitude thin cirrus and its strong dependence on ice water content. For example, they calculate that for a .0002g/m^3 ice water content (6.7 e^{12} mol/cc), a 3 km thick cloud provides about 1.5 W/m^2 of infrared heating, and this heating scales directly with ice water content. McFarquhar et al. [2000] report cloud radiative forcing calculations using microphysical and lidar data during the Central Equatorial Pacific Experiment averaging 1.58 W/m^2. One of the primary goals of CF is to develop the capability of modeling the radiative properties of thin cirrus starting with space-based millimeter wave measurements of ice water paths within the cloud. Testing this capability first requires accurate in situ measurements of the microphysical properties of thin cirrus with simultaneous or nearly simultaneous measurements of the cloud reflectivity. Measurements of the potentially small ice water content of thin cirrus need to be accurate and precise enough to adequately constrain models calculating the radiative properties of these clouds because this additional heat source could measurably impact the slow ascent rates in the upper tropical troposphere.

Total water measurements are also critically important for understanding the water vapor budget of the upper troposphere and lower stratosphere. Quantitatively determining the fate of ice convectively transported to the upper troposphere, that is what the profile of evaporated ice from these convective systems, requires a measurement of cloud ice water content. This requires synergy between remote instruments that provide the overall cloud image and in situ instrumentation that can be used to quantify the ice water distribution seen in the cloud.

As detailed in the SPARC report of 2000 [SPARC, 2000], stratospheric water vapor has increased by about 2 ppmv since the 1950s. While half of this can be attributed to the increase in methane, which is oxidized to water vapor, the source of the other 1 ppmv remains a mystery. What exacerbates the problem is our lack of a detailed understanding of the mechanisms that control entry-level stratospheric water vapor. Whether the dominant mechanism is convectively driven or involves dehydration during slow ascent, accurate measurement of the ice water content associated with thin cirrus clouds potentially involved in the dehydration process is critical. For example, if water vapor condenses as an air parcel is cooled, water vapor obviously decreases while total water remains the same. On the other hand, if the source of a cirrus cloud is an anvil, there is no constraint on the total water in the cirrus cloud relative to the water vapor in the

surrounding cloud-free air. As a result, the conservation of total water can be used as a test for distinguishing a cloud formed in situ from one resulting from anvil formation.

The total water instrument can be viewed as a close relative of a water vapor instrument, with each utilizing an identical module for detecting ambient water vapor, but different inlets. The water vapor inlet is designed to be "wall-less", and deliver ambient air to the water vapor detection module without contamination from instrument walls. It must also avoid evaporating ice particles or water droplets. A total water instrument needs to deliver ambient air to the detection module that has fully evaporated ambient ice particles, to maintain ambient ice particle densities using isokinetic flow, or if necessary use anisokinetic flow and accurately calculate particle enhancements, and in either case avoid contamination from instrument walls. In cloud-free air, each instrument should identically measure ambient water vapor, and this represents a first-order requirement for validating the accuracy of a total water instrument. Because the two instruments operate in different flow regimes and at different temperatures, this criterion actually poses a strict test on the data quality of both instruments. Furthermore, intercomparison in cloud-free air with the JPL open cell tunable diode laser infrared absorption hygrometer [May et al., 1998] further adds to the validation process for the instrument pair. Nevertheless, recent history indicates that validating the accuracy of water vapor instruments to the satisfaction of the broad community of interested atmospheric scientists remains challenging.

Figure 1 in the SPARC Assessment of Upper Tropospheric and Stratospheric water vapor (SPARC 2000), the bottom third of which is reproduced as figure 1 here, presents a summary of relationships between stratospheric water vapor measurements from different instruments. We quote from the conclusion section of chapter 2 on data quality, with specific reference to this figure, "For both the troposphere and stratosphere there is no single technique or instrument platform that is recognized as a standard to which other techniques should be compared, and thus comparisons were made relative to one another". In other words, after about thirty years of instrument development, testing, validating, and intercomparing, it is unclear whether we are making water vapor measurements accurate enough to satisfy the needs of the scientific and global communities. For example, the reported trend in stratospheric water vapor previously mentioned is thought to be a prominent indicator of climate change. Accordingly a reported increase of 1%/year over a 45 year period must be taken seriously. Nevertheless, considering the volatility surrounding global climate change and proposed governmental responses to that change, and the state of water vapor measurements as reported in SPARC 2000, how much credibility can be given to the data sets used to determine that trend? Solutions to additional questions regarding testing strat-trop exchange mechanisms, measuring supersaturation in and around cirrus clouds, or predicting heterogeneous ozone loss in polar regions, require water vapor measurements with proven accuracy. In order to avoid instrument dependent conclusions, a "standard" or "benchmark" water vapor instrument is required. Additionally, while the in situ instruments on the NASA ER2 research aircraft, namely those from Harvard and JPL, agree with each other very well [Hintsa et al., 1999], in Figure 1 they appear to be systematically higher than the other instruments, with the average difference from HALOE about 20%. This provides the average reader with the impression that measurements by these two in situ instruments are significantly biased high.

The determination of cloud ice water content by subtracting the water vapor measurement from the total water measurement depends on the calibration and validation of each of the Harvard water instruments. If the implications of Figure 1 that is adapted from the SPARC report

are not addressed, our validation efforts for the total water instrument and the accurate determination of cloud ice water content are in vain.

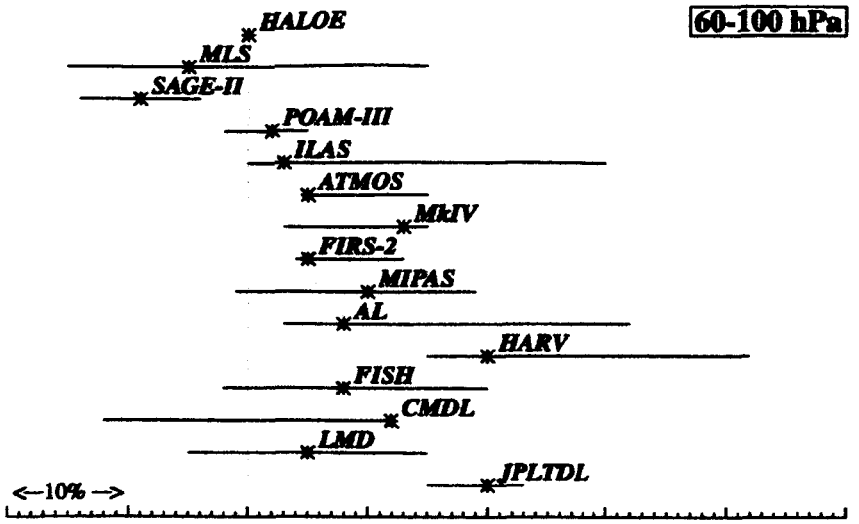

Figure 1. Reproduction of the bottom third of Figure 1 of the SPARC 2000 report. Data is plotted for each instrument as % difference from HALOE determined either from direct intercomparisons, represented by asterisks, or indirect comparison, represented by a horizontal line covering the range of disagreement. If the asterisks is centered in the line, it represents the average of the indirect intercomparisons.

History of Total Water Instruments

There have been only a few instruments developed to measure total water in the UT/LS, and details of inlet and heater design are often unpublished. Kelly [1993] utilized a pair of Lyman-alpha photofragment fluorescence hygrometers with forward and rear-facing inlets contained within an aerodynamically shaped pod (football) suspended from the fuselage of the NASA ER2 research aircraft. Water detection coupled with a forward facing inlet measured total water while that coupled with the rear-facing inlet detected only water vapor. The air is heated to 60°C to evaporate particles. Flow in the total water instrument was not isokinetic, so corrections were made to the ice water concentration based on the calculation of flow through the instrument relative to that of the ambient free air stream. Schiller et al. [1999] reported results from a total water instrument on board the DLR (Deutches Zentrum fur Luft- und Rumfahrt) Falcon research aircraft. The instrument was a modified version of the FISH instrument [Zöger et al., 1999] that utilizes Lyman alpha photofragment fluorescence detection and an inlet with anisokinetic flow to enhance sensitivity to low ice water. A stainless steel inlet tube is heated to 80° C for particle evaporation. It uses measured particle size distributions from a multi-angle aerosol spectrometer probe along with fluid dynamical calculations to determine enhancement factors.

Similarly, Avallone has developed a total water instrument that flew on the NASA DC-8 research aircraft during the SAGE Ozone Loss Validation Experiment (SOLVE) in 2000, and more recently on the aircraft during CF. The instrument uses a single pass Infrared Diode Laser Spectrometer for detection [MayComm Instruments, LLC], a heated inlet, and anisokinetic flow to enhance sensitivity to thin ice clouds. Webster et al. (2003) have modified the Aircraft Laser Infrared Absorption Spectrometer (ALIAS), designed for measurements of HCl, N_2O, CH_4, NO_2, and HNO_3 [Webster et al., 1994], for the measurement of total water and its isotopes. It combines a heated inlet with isokinetic flow and multipass infrared absorption to simultaneously measure total water and its isotopes. The total water instrument that we developed is differentiated from most of the aforementioned instruments because it measures total water with an isokinetic inlet. In principle, the enhancement factor in anisokinetic particle sampling can be calculated, and asymptotically reaches a value approximately equal to the ratio of ambient and inlet mass flows

for particles larger than about 20 microns. However, for a range of particle sizes prevalent in thin cirrus, with median particle diameters of 5-10 microns, for which this instrument was designed, calculated enhancement factors may have unacceptably large uncertainties. The modified ALIAS instrument also has an isokinetic inlet, but intercomparisons in clear air during the CF mission suggest that in its first science mission it suffered from significant wall contamination and hysteresis effects.

While all the aforementioned instruments measure total water, one instrument, using a counterflow virtual impactor for particle sampling [Twohy et al., 1997], directly measures cloud ice and/or liquid water content. This instrument has previously flown on the NCAR Electra and Cessna Citation operated by the University of North Dakota, with peak altitudes of about 40,000 feet. It is in the process of being integrated onto the WB-57 for cloud studies as well as intercomparison with the previously described total water instruments.

In the next section we focus on instrument accuracy, followed by sections on instrument details, laboratory calibrations, and instrument performance, including in-flight absorption measurements and instrument intercomparisons.

Total water instrument details

The total water instrument was designed to fit into a 1-meter wide pallet that is hoisted in place to become part of the underbelly of the WB-57 fuselage. Figure 2 illustrates the instrument as it is mounted in the pallet. The picture illustrates the location of the inlet, extending almost a meter out from the edge of the pallet that is roughly 1.8 meters wide. The inlet is firmly supported by weldments that are bolted to struts at the bottom of the pallet. An aerodynamically designed aluminum clamshell is bolted to the inlet and the entire assembly is sealed with low temperature RTV silicone sealant. Once assembled in the pallet, the instrument can remain there for the entire mission, because the pallet system is designed to allow easy access to all of the instrument components therein. As configured in Figure 2 for test flights and the CWVCS mission, the pallet also contains the Harvard ozone instrument. For the CF mission, the instrument was reconfigured to allow room for the Harvard carbon dioxide instrument [Boering et al., 1994].

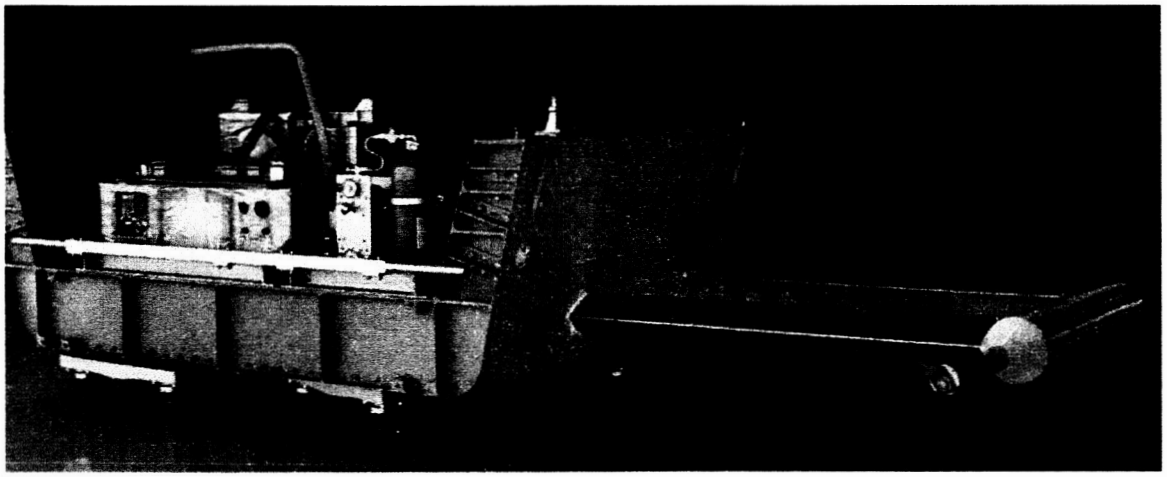

Figure 2. The total water instrument in flight configuration mounted in WB-57 pallet in preparation for a flight at NASA Johnson Space Flight Center.

The detection scheme for the total water instrument is based on the same principles as the water vapor instrument [Weinstock et al., 1994], and is intended to fly in conjunction with it. As

illustrated schematically in Figure 3, the total water instrument can be divided into four subsystems:

1. A carefully designed and positioned inlet through which solid water particles are brought into the instrument duct such that the quantitative relationship between ambient ice water content and sampled ice water content of air is determined to better than 10% for particle sizes up to 100 μm in diameter. A shroud is used to straighten the air streamlines as they approach the inlet. The shroud helps compensate for the WB-57 angle of attack that is approximately three degrees at cruise but increases slightly during ascent and descent.
2. A heater that efficiently and completely evaporates the solid/liquid water before it reaches the detection axis.
3. Ducting through which the air flows to the detection axis without perturbing the water vapor mixing ratio.
4. A detection axis that accurately and precisely measures the total water content of the ambient air.

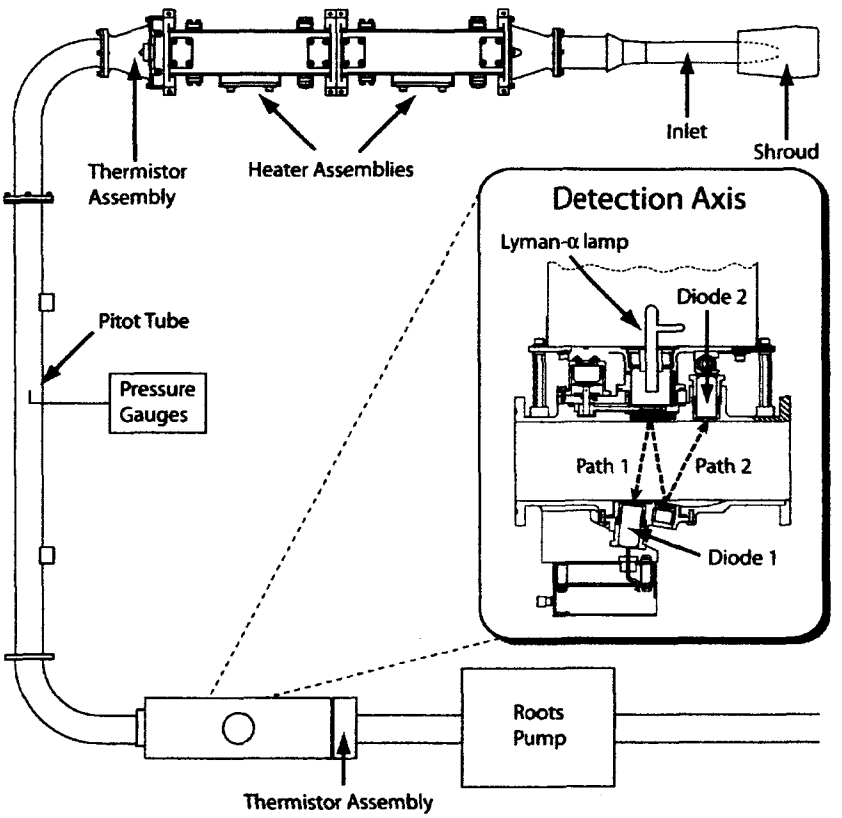

Figure 3. A schematic representation for measuring total water by photofragment fluorescence. The detection axis illustrates the Lyman-α lamp, absorption paths, and photodiodes. The photomultiplier and associated optics for fluorescence detection that sits at right angles to the exciting light and air flow is not shown here.

The accuracy of the instrument depends on how well the instrument performs each of the four functions described above. Instrument uncertainty, discussed below, can be determined by properly combining the uncertainties in the performance of each of those functions. We will discuss each of these instrument subsystems separately.

The Inlet

There are three basic considerations for designing the total water inlet: (1) the position of the inlet relative to the aircraft skin, (2) the inlet shape, and (3) the angle of attack. The ultimate question for all three aspects is how do the trajectories of particles entering the inlet vary as a

function of particle shape and size, and how will perturbations of particle trajectories affect the relationship between sampled particle density and that in the ambient air stream. In all cases the momentum of the particle tends to keep it moving in a straight line even as the gas streamlines are bending to avoid obstructions such as the aircraft fuselage or the inlet nose. Measurements have shown [King, 1984], that for a range of aircraft, aircraft velocities, and ambient pressures enhancement factors depend on a modified Stokes number, S, where $S = 2a^2v\rho_p/9vr$, and d/b, the ratio of the inlet distance from the fuselage to the fuselage radius. Here, a is particle radius, v is flow velocity, r is fuselage radius, ρ_p is particle density, and ν is viscosity of the air. The enhancement factor can be calculated for values of S up to 6 (maximum enhancement), using empirical equations from King [1984]. We plot in figure 4a particle enhancement factors for a fuselage radius of about 1 meter and a value of d/b = 1, as a function of S. With d/b = 1, or a 1 meter distance from the aircraft skin, particles can be measured with an enhancement of 6% or less. Figure 4b illustrates the enhancement as a function of d/b for $S = 6$.

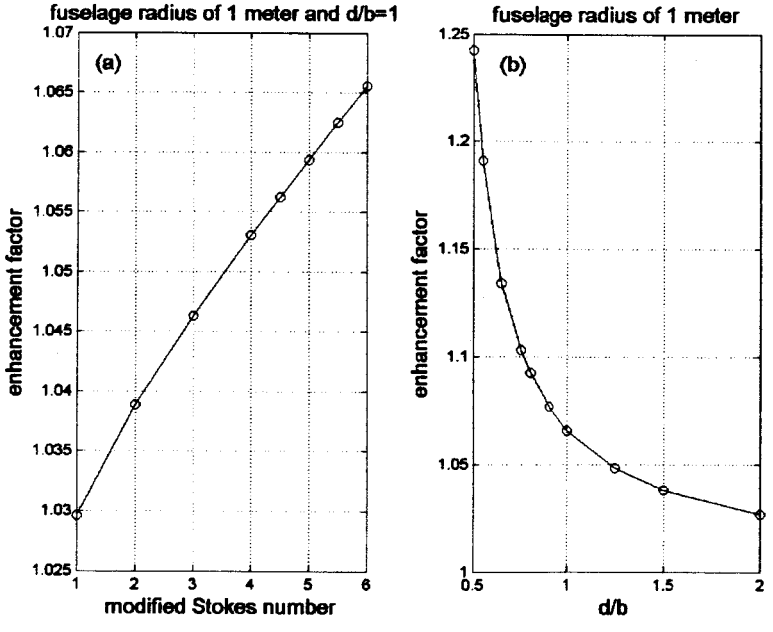

Figure 4. Plots illustrating the efficiency of measuring particle density on the inlet designed for the WB-57. In (a) the particle enhancement factor is plotted *versus* the modified Stokes number. In (b), the variation of enhancement factor is shown as a function of inlet distance from the aircraft divided by the aircraft radius for $S = 6$, corresponding to 50 μm diameter particles.

Theoretical and experimental studies of air flow and particle trajectories around aircraft fuselages [King, 1984; King et al., 1984] indicate that for quantitatively sampling particles up to 50 μm diameter, the inlet must be separated from the skin of the aircraft by a distance equal to the aircraft radius at the inlet attach point. These calculations have also been carried out [King, 1985] for ice particles of variable shape and ice density, with the results consistent with those assuming spherical water drops. That is, dependence of the enhancement factor on a modified Stokes number is independent of particle shape. However, the enhancement factor does depend on ice density, which is typically not well known for large ice particles. From these calculations and the value of d/b = 1 for the position of the total water inlet on the WB-57, we estimate that the enhancement caused by the flow of streamlines around the fuselage is about 7% in fairly thick cirrus. This is the enhancement value when $S = 6$. In thin cirrus, where smaller particle diameters lead to a lower modified Stokes number, the enhancement should be less than 4%.

The requirement of isokinetic flow means that the mass flow at each point across the inlet must be identical to the corresponding ambient mass flow. With a nozzle inner diameter (id) of 1

cm, the velocity through the 2" square cross section detection axis will be about 5–6 m/sec when the flow is isokinetic, depending upon the true air speed of the WB-57. A Roots pump is used to both regulate this velocity in response to changes in altitude and velocity, and scan flow velocity for diagnostic purposes. The control circuitry for the Roots pump uses the pressure, temperature, and true air speed as supplied from aircraft navigation data to set the pump rpm. Laboratory calibrations in the flight duct over a range of pressures are used to set the relationship between rpm and pump throughput. Measurement error is proportional to the anisokinetic factor, A, defined as the ratio of the integrated mass flow through the 1-cm id cross section inlet to the mass flow of the free air stream through a comparable cross sectional area, where oversampling (undersampling) with $A > (<) 1$ leads to an under (over) determination of ice water content.

The errors incurred in establishing isokinetic flow are threefold. The first is in our laboratory determination of the mass flow within the inlet, and mostly results from the uncertainty in the relationship between the pitot tube differential pressure measurement and the mean flow velocity. The second is in the ambient mass flow based on the assumption that the aircraft navigational velocity, pressure and temperature are suitable substitutes for the actual velocity, pressure and temperature at the inlet. The third is that the flow field is constant across the 1-cm id cross section of the inlet. Because our inlet is located underneath the fuselage centerline, and accordingly below the wing, there is the likelihood that ambient pressure at the inlet is higher than measured aircraft pressure. Three-dimensional computational fluid dynamics calculations [Engblom and Ross, 2003], carried out at angles of attack of two and six degrees, indicate that the Mach number at the inlet is reduced by 9% and 15%, respectively, while the pressure is increased by 1.5% and 5%, respectively. When combined, these changes at our inlet suggest we are undersampling particles larger than about 20μm diameter by 3.5 to 11% depending on the aircraft angle of attack. While the undersampling is small, especially at cruise, it does work in opposition to the oversampling caused by the airplane fuselage shadow effect. The degree to which this impacts our measurement is intimately related to the design of the inlet and how it affects particle sampling under anisokinetic conditions.

The NACA 1-55-100 inlet shape is used for the 1-cm id inlet [Soderman et al., 1991]. It has been proven by wind tunnel tests that to avoid flow separation or measurement enhancements it is necessary to attack the streamlines within an angle of a degree or two. As shown in the wind tunnel test of Murphy and Schein [1998], a shroud around the inlet allows flow at the inlet entrance to be significantly less sensitive to this angle. For our inlet, the shroud is 3" id, and is scaled directly from the inlet used by Murphy and Schein. Using Rader and Marple (1988, equation 17), we calculate that the sampling efficiency scales inversely and approximately linearly with absolute value of the mass flow ratio, with a ratio of 1.1 (or 0.9) giving a 10% undersampling (or oversampling). Accordingly, depending on aircraft angle of attack, we estimate a maximum –4% to –11% enhancement from flow perturbations at the inlet, which fairly well cancels the particle enhancement caused by the aircraft fuselage. While these calculations provide some confidence in our particle sampling efficiency, it would be preferable to validate in flight that we are sampling isokinetically or close to it. For this reason during the CRYSTAL FACE mission we programmed the instrument to dither the roots pump rpm such that our duct velocity was varied from 75 % to 150% of it's the nominal isokinetic value for short periods of the flight. Because of the variability in the ice water content of clouds, testing the inlet efficiency requires a comparison with other instruments on the aircraft. During the CRYSTAL FACE mission there were two other instruments that measured total water. One, is a closed-path tunable

diode laser hygrometer (CLH), coupled to a heated, forward-facing inlet that provides high sensitivity during thin cirrus events with anisokinetic sampling. The other, the Airborne Laser Infrared Absorption Spectrometer (ALIAS), uses an isokinetic inlet and heated duct modified to measure total water in its various isotopic forms. Unfortunately, there were no opportunities to investigate the sensitivity to flow velocity by intercomparing with the other total water instruments.

The Heater

The heater design is predicated on the need to completely vaporize 100 μm diameter particles within the transit time from the heater to the detection axis, about 160 milliseconds when the aircraft velocity is 150 m/sec. Based on typical ambient temperatures and pressures in the upper troposphere and lower stratosphere, a 600 watt heater is needed to raise the air temperature to about 30° C. The heater consists of two 300 watt assemblies that are wired in parallel and constructed of strips of nichrome ribbon, (California Fine Wire Stableohm 650, 0.004" thick, 0.25" wide, with a resistance of 0.55 ohms/ft) mounted axially in the flow tube, providing extremely efficient heat transfer to the air stream. The assemblies are mounted in a 1.25" id section of the flow tube. A set of three thermistors just downstream of the heater monitor the air temperature with the center thermistors providing a signal used in a feedback loop by a pulse-modulated heater controller that maintains the air temperature stable to better than a degree. While the three thermistors, indicate a temperature gradient between the wall and the center of the tube of about ten degrees/cm, it is the temperature of the core that is most important. This is because while the ducting expands from the initial 1-cm id of the inlet to a 5-cm rectangular cross section at the heater, the trajectories of the larger particles are preferentially maintained in the central core of the flow.

During the CF campaign, we encountered cirrus clouds with particle diameters up to a mm, significantly larger than the 100 μm diameter the instrument was designed to evaporate. While the potential of incomplete evaporation of large particles is significant, especially based on evaporation times for these particles in a duct maintained at 30 °C, the actual temperature of the core of the flow as it passes through the 30-cm long heater is much higher than the duct temperature. We first illustrate in figure 5 the evaporation time in the duct as a function of particle size, using equation 13.19 from Hinds [1999]. In the top panel we see that evaporation times are well in excess of the 160 msec residence time of the instrument but it is also noteworthy that by raising the temperature to 60°C we can fully evaporate particles of about 250μ diameter within 160 msec. This temperature increase will represent the simplest change in instrument operation for future missions in which thick cirrus will be sampled.

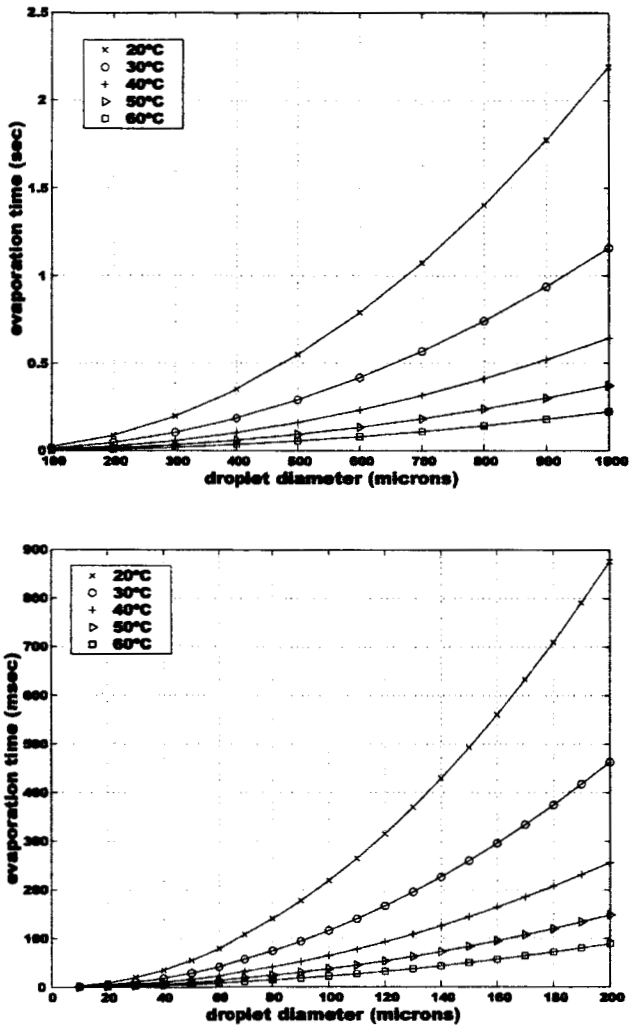

Figure 5. Evaporation times plotted for various particle sizes up to 1000μm diameter (top) and up to 200μm (bottom) as a function of duct temperature.

The instrument detection axis fortuitously affords us an opportunity to evaluate evaporation efficiency. Both the water vapor and total water lamps emit 309 nm radiation that is detected by the fluorescence PMT as a result of surface and molecular scatter. Accordingly, when the WB-57 passes through a cloud, the PMT shows a clear signal that is proportional to the particle density in the cloud. If the particles solely undergo evaporation in the heater and duct, then that signal can be expressed as $S = KFd\tau$, where K is a proportionality constant, F is the photon flux from the lamp within the bandpass of the optical filter, d is the particle density, and τ is the residence time of the particle within the lamp beam. To first order, the sensitivity to particle scattering is the same for the total water and water vapor instruments allowing us to assume the same KF for both instruments. The residence time for each instrument is inversely proportional to the duct velocity, which is 5-6m/sec for total water and about 80m/sec for water vapor. Therefore, scattering in the total water instrument should be at least ten times that in the water vapor instrument for the same cloud particles. With this assumption, the fraction of unevaporated particles is negligible.

However, we must now consider the possibility that the particle undergoes melting along with evaporation. Using equations 16-76 and 16-77 of Pruppacher and Klett (1997) we calculate that the melting time for 100–500 micron particles in the duct is on the order of a few tenths of a second. These equations somewhat underestimate the rate of melting [Rasmussen et al., 1984] but are adequate for our purposes and suggest that the ice particles in the total water duct undergo simultaneous evaporation and melting. During the transit time in the duct, it is likely that partially melted particles collide with the walls at two right-angle turns, during which the liquid component sticks to the wall, where it quickly evaporates, and the frozen component bounces off. It is likely that further melting continues after the last wall collision so that the remaining ice particles have an ice core but are liquid at the surface when they reach the detection axis. To check this assumption, we have measured the scattering signal from a stream of 70 μ droplets falling through the detection axis where they encounter a photon flux consistent with that used in flight. We compare the resulting scattering signal, equal to about 25 counts/(second-particle), with the scattering signal observed for a specific case during the 20020729 flight when ice water derived from particle measurements is significantly higher than measured by our instrument. While we find that the assumption of spherical droplets requires too high a percentage of the ice water to remain unevaporated, the agreement is close enough to suggest that the particles remaining are in fact liquid on the surface, but most likely are not spherical and remain more efficient scatterers than liquid drops.

Because of the ambiguity regarding the phase of the particles remaining at the detection axis, total water measured during CRYSTAL FACE flights for which there is a sizeable scattering signal must be viewed as a lower limit. We will outline planned changes to the instrument to remedy this problem later in the manuscript.

The Roots Pump

Laboratory pressure drop tests through a prototype total water instrument indicated that the use of aircraft ram pressure would be insufficient to maintain isokinetic flow. A roots pump was chosen because of its capability of pumping a great deal of air without the need to maintain a significant pressure drop. The Eaton Supercharger Model 45 (Magnuson Products, Ventura, CA) was chosen in part because of its previously successful use at low pressure (Darin Toohey, private communication). The pump was typically run between 2000 and 3000 rpm providing a displacement of about 40 to 60 CFM. The pump is controlled by a combination Parker NO342FENMSN brushless servomotor and a Parker Automation Gemini GVU3 120/240VAC digital servo controller. During the first test flight series in May 2001 as well as the science mission in August 2001 in San Jose, Costa Rica, the pump rpm was systematically varied from 1500 to 3000 rpm, providing flow from approximately 10% below to 25% above the isokinetic velocity in order to evaluate instrument sensitivity to flow velocity, especially in clear air. For the CRYSTAL FACE mission, with the goal of having isokinetic flow, the rpm of the pump was actively controlled, using an algorithm that calculated required mass flow from NAV pressure, temperature, true air speed, duct temperature, pressure, and flow velocity. The duct flow velocity was determined from the tube differential pressure as measured by a pitot-static pressure tube (United sensor # PCC-12-KL) modified to mount in the flow tube and validated in the laboratory over a wide range of pressures and flow velocities.

The Detection Axis

The detection axis is functionally identical to that in the water vapor instrument that has been previously described in detail [Weinstock *et al.,* 1994]. A simple diagram is shown as part of

Figure 2. Briefly, 121.6 nm (L_α) radiation from an RF discharge lamp photodissociates water vapor in a 2-inch duct. A fraction of the resulting OH fragments are formed in their first excited electronic state ($A^2\Sigma^+$), and the OH fluorescence at ~315 nm is collected at right angles to the L_α beam through a narrow-band filter and detected with a photomultiplier tube (PMT). Because the fluorescence is strongly quenched by collisions with O_2 and N_2 at a rate proportional to the air density, at altitudes of the upper troposphere and lower stratosphere the observed detector signal is proportional to the water vapor volume mixing ratio. Lamp scatter near 315 nm is measured by using a quartz window to periodically block the L_α beam. Changes in lamp intensity monitored with a vacuum photodiode opposite the lamp are used to normalize the fluorescence signal. Additionally, a 25.4 cm focal length, 12.7 cm diameter rear-surface mirror, coated for the vacuum ultraviolet, is used to reflect a portion of the L_α beam back across the tube to a second photodiode, providing the means to carry out in-flight absorption measurements when the water vapor concentration is sufficient, typically in the mid- to upper troposphere.

Instrument Performance and Evaluation

Engineering flights for the total water instrument took place in May 2001 from the NASA Johnson Space Flight Center at Ellington Field, Houston, TX. All subsystems of the instrument performed very successfully providing the opportunity to evaluate how well the instrument measures water vapor in cloud free air and total water in a cloud. In either case the minimum success criteria are that the total water mixing ratio at the detection axis equals ambient total water and that the detection sensitivity to water vapor in flight is the same as that established by laboratory calibrations. Passing these criteria need to be addressed independently in both clear air and clouds. We address the calibration question first, because it bears on the accuracy of all the measurements by both instruments. We then follow with validation using in-flight absorption measurements and finally intercomparison with other instruments on the WB-57.

Instrument calibrations

The pre- and post-mission laboratory calibrations are carried out for the water vapor and total water instruments by flowing known mixing ratios of water vapor through the detection axes [Weinstock *et al.,* 1994]. Saturated air-water mixtures are prepared by passing air through a two-stage bubbler apparatus. These are diluted with additional dry air before being sent to the detection axes, which are integrated into the laboratory flow system. As in the past, the calibrations explore both a wide range of water vapor mixing ratios (20–500 ppmv) and pressures (20–300 mbar) in order to determine the instrument calibration and validate its operation throughout the full range of conditions seen during a flight. However, the use of temperatures corresponding to ambient conditions in flight has never been a consistent part of the calibration procedure. This was a valid concern for the Harvard water vapor instrument, in which detection axis temperatures are typically about 20°C degrees above ambient, but typically about 80°C below room temperature. Potential sensitivity to gas temperature exists because OH molecules formed in a range of rovibronic states as part of the photofragment fluorescence process undergo collisonal deactivation. The rate of this process could have a significant temperature dependence that would perturb the fluorescence efficiency. For this reason, as described in Weinstock et al., [1994], and Weinstock et al. [1990], laboratory experiments were carried out to verify no significant dependence of the calibration on duct temperature. Nevertheless, because the air temperature at the total water detection axis is only about 10°C, any uncertainty in the calibration resulting from air temperature is virtually eliminated.

Accordingly, typical agreement of 3% or better between water vapor measured by the water vapor and total water instruments validates the lack of temperature dependence of the photodissociation process that defines the sensitivity of the detection axis. However, agreement also depends on the stability of the calibrations of the two instruments and/or our ability to track each instrument's sensitivity throughout the field mission. Typically, optical degradation not only tends to decrease instrument sensitivity during the mission by reducing the flux of 121.6 nm radiation, it also complicates our accurate measurement of that flux. The variability or uncertainty in the agreement can also be limited by the signal-to-noise of each instrument, especially when measuring low water vapor mixing ratios. The signal to noise of both the water vapor and total water instruments are not limited in any fundamental way. However, optical and surface degradation often reduce each instrument's signal-to-noise during a mission.

In-Flight Absorption Measurements

Absolute accuracy to 5% is a critical performance criterion for water vapor measurements. Measurement of water vapor at he detection axis by in-flight absorption specifically tests or validates the absolute calibration of the detection axis at the temperature and pressure in the duct. For this measurement, carried out exactly as in the water vapor instrument flown simultaneously on the WB-57 as well as the one that has flown on the ER-2, a 2-sigma error of 5% has been quoted. Realistically, this quoted uncertainty might have to be increased for any given data set when optical degradation from salts dissolved in cloud ice cause the instrument sensitivity to change from flight to flight. While this can be somewhat accounted for by laboratory calibrations carried out in the field, less than ideal conditions along with time constraints limit the utility of this approach and alternative approaches to tracking the relative sensitivity of the water vapor instrument in flight are being explored. Fortunately, the same abundance of clouds sampled during flights that exacerbated optical degradation problems, facilitated repeated in-flight validation of the total water calibration. This approach, is identical to that used for in-flight validation of the Harvard water vapor instrument during the STRAT and POLARIS campaigns [Hintsa et al., 1999], and accounts for any changes in lamp intensity [Kley et al., 1979, Weinstock et al., 1994] by simultaneously utilizing two absorption path lengths. In figure 6 we show two typical examples of in-flight absorption measurements during the CRYSTAL FACE campaign. These both show that water vapor by absorption is measuring about 7% higher than that measured by fluorescence.

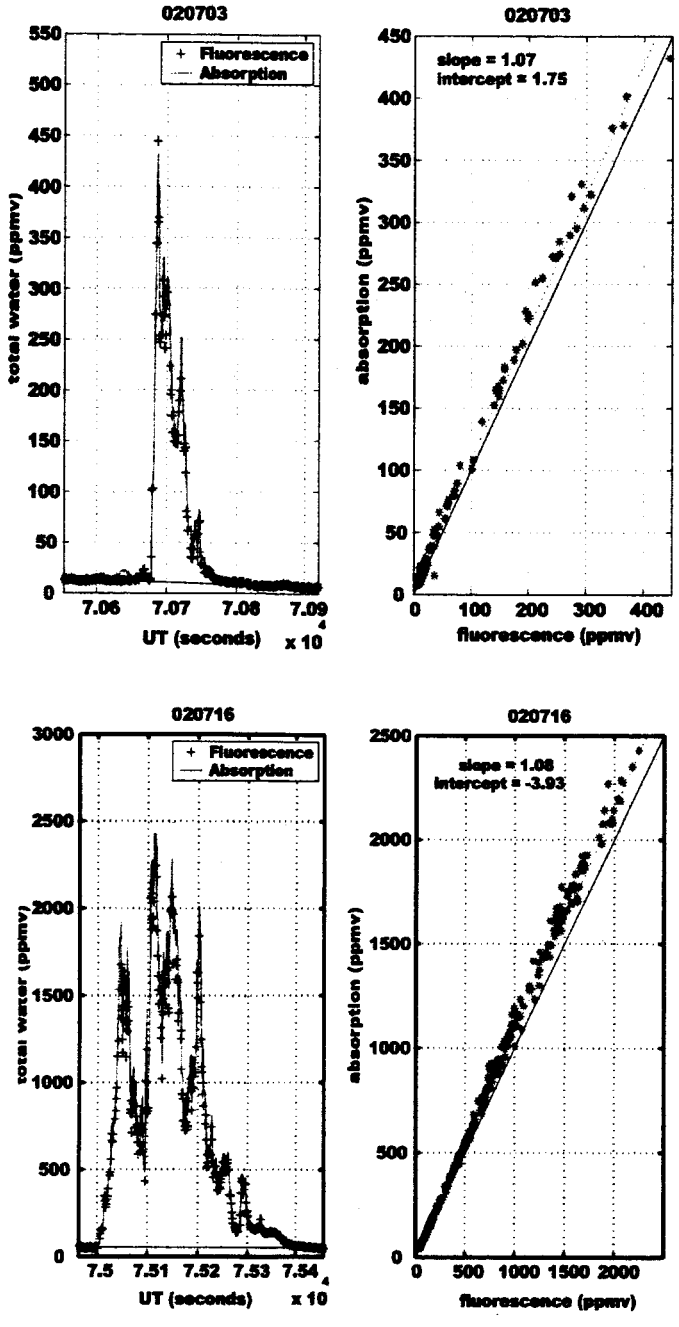

Figure 6. Sample in-flight intercomparisons during the July 3 and 16, 2002, flights. The left-hand panels shows the detailed agreement between total water measured by absorption and fluorescence. The right-hand panels plot water vapor measured by absorption *versus* fluorescence for the same data points plotted in the left-hand panels, as well as a linear least squares fits to the data (dotted line). Also plotted are the slope = 1 lines for reference.

In Figure 7 we look at all the in-flight absorption intercomparisons during the flights from Key West in July. The fit to all the intercomparison data made during five flights indicates that agreement between the two methods shows an apparent statistical variability of about 5%, and that an apparent change in instrument sensitivity took place between the flights on July 16 and

July 23. Field calibrations, albeit limited in number, do not show this change, and we have not accounted for the implications of this change in the flight data analysis.

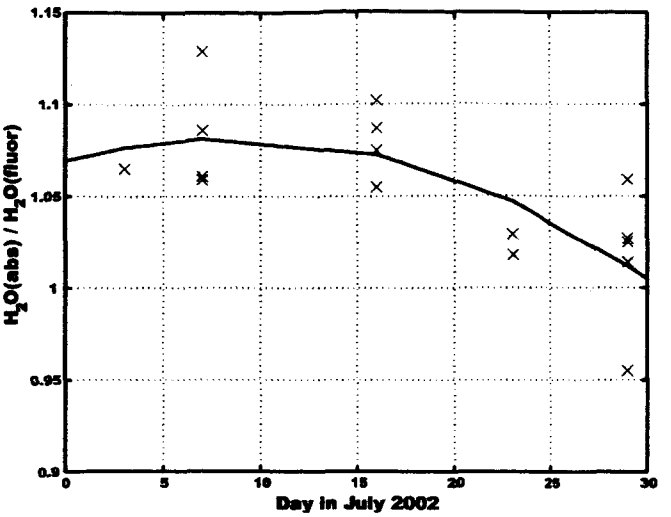

Figure 7. Plot of a polynomial fit to the results of all the total water in-flight absorption *versus* fluorescence intercomparisons. Each point represents the slope of a least squares fit to the intercomparison data as shown in Figure 6.

For reference we include in Figure 8 an example of a similar intercomparison for the water vapor instrument. There were very few opportunities for in-flight intercomparisons for the water vapor instrument, with this example providing the most stable background on either side of the absorption feature. This intercomparison is consistent with the total water intercomparisons.

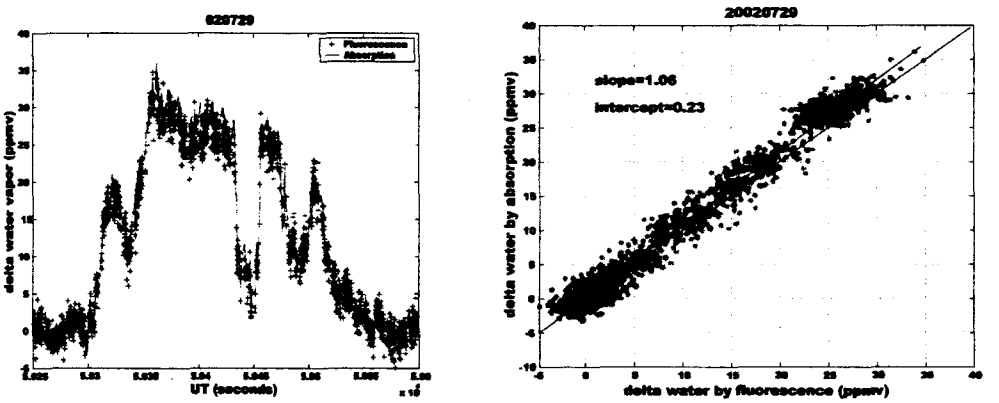

Figure 8. As in Figure 6, but for water vapor during the 20020729 flight.

Intercomparisons of Harvard Total Water with Harvard and JPL Water Vapor: Clear Air

An independent measurement of water vapor is needed along with the total water measurement to determine the ice water content of the sampled cloud. The Harvard University water vapor instrument can serve that purpose and is also invaluable to validate the total water measurements in clear air, a necessary step before evaluating its measurement in clouds. While the detection axes for the two instruments are virtually identical, the instruments operate in very different flow regimes. The water vapor instrument flow rates are typically about 60–80 meters/sec in a 5-cm rectangular cross section duct, providing a mass flow more than ten times that in the total water instrument. Accordingly, outgassing from instrument walls and hysteresis

effects that are not an issue in the water vapor instrument become a significant concern for the total water instrument.

We show in Figure 9 water vapor measurements from the first test flight, on May 21, 2001, where total water is plotted against water vapor. While agreement between the two instruments is typically better than 10%, this can be somewhat misleading. While the scatter in the data would appear to be acceptable, a closer look at the data is required. We show in the top panel of figure 10b water vapor plotted *versus* time as measured by the two instruments. In the remaining panels are plots of ambient temperature and pressure. Regardless of the absolute sensitivities of the two instruments, there are clearly three different regions that display evidence of hysteresis, in which walls and surfaces either act as sources or sinks for water vapor. The most obvious occurs at the beginning of the flight, where total water measures high, presumably as the walls outgas during ascent. Because the aircraft ascended through fairly thick cirrus, as indicated both visually and by the total water measurement, this could be an additional factor. If a small fraction of cloud water sticks to instrument surfaces, especially upstream of the heater, or prior to the heater being turned on, this water could later outgas when ambient water and pressure decreases. The other feature, when total water measures lower than water vapor, occurs during measurements of the lowest water vapor mixing ratios, and the discrepancy appears to anti-correlate with ambient temperature, although there does appear to be a lag time as well. We hypothesize that this represents the sticking of water vapor to the insufficiently heated inlet walls when its temperature is below ambient. The third region to focus on is in the middle of the flight where total water lags water vapor both as water increases and again as it decreases. The hysteresis here appears fairly benign and can only properly analyzed when directly compared to the water vapor instrument measurement.

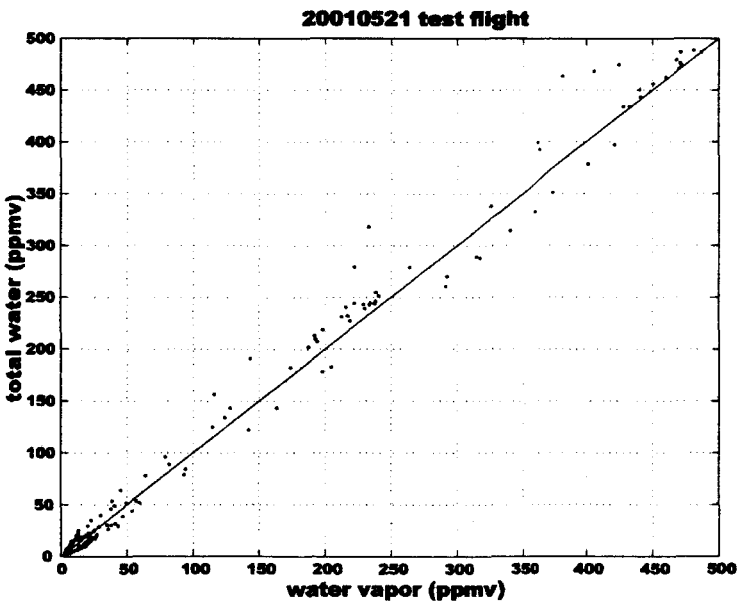

Figure 9. Plot of total water *versus* water for the test flight out of Houston on May 21, 2001, illustrating general overall agreement of the two instruments for measuring water in clear air. The 1:1 line is added to illustrate agreement.

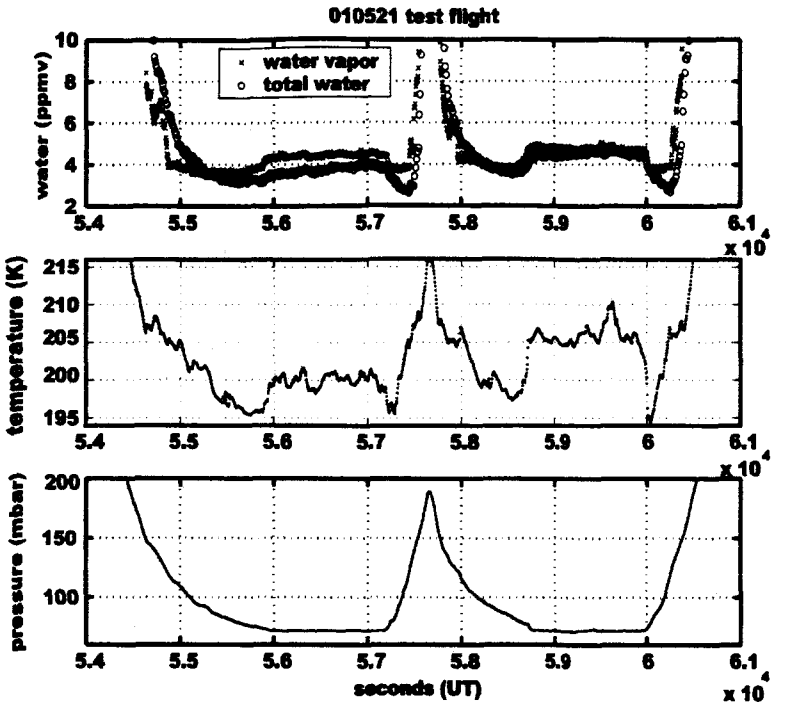

Figure 10. The top panel shows under close inspection the small systematic differences between the water vapor and total water instruments during the May 21, 2001 flight as described in the text. The middle and bottom panels are plots of temperature and pressure *versus* time during the flight.

It is important to comment that the type of behavior exhibited here is insidious and prevalent in *in situ* instruments that measure molecules that adhere to surfaces, not only water vapor. Furthermore, by comparing the "agreement" illustrated in Figure 9 with the "disagreement" illustrated in Figure 10 using the exact same data, we make the point that scatter plots can obfuscate rather than illustrate the actual agreement or disagreement in data sets. It is also necessary to stress that making accurate water vapor measurements in clear air is a necessary but not sufficient condition for validating the accuracy of the total water measurement in clouds. The degree to which the instrument exhibits hysteresis directly impacts its accuracy. To further illustrate this point we focus on a section of the 20020716 flight during CF, where the traverses the same thick cirrus cloud three times, with measurements of total water reaching more than 2500 ppmv in the cloud, and with background water vapor about 30–35 ppmv. In the top panel of figure 11 we show water, total water, and the ice water content derived from the Multi Angular Spectrometer Probe (MASP) [reference MASP] as the WB-57 traverses the cloud, focusing in the bottom panel on the water values at the edges and outside of the clouds. We use the MASP data to clearly delineate the cloud edges, with arrows pointing to times after cloud traversals where the water vapor measurement by the total water instrument is clearly high. This extreme case illustrates the limited impact of the walls even in this region where the ice water content of the cloud is up to 100 times the background water vapor.

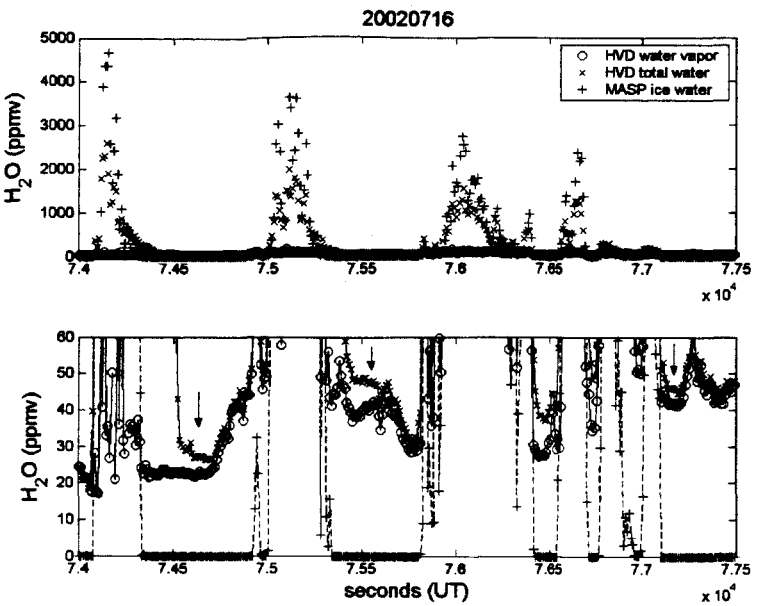

Figure 11. Plots of water vapor and total water made during the July 16 flight over Florida *versus* time. The vertical scaling in the bottom panel facilitates focusing on the regions of hysteresis denoted by the arrows. The MASP ice water content measurement can be used to mark cloud edges.

On the other hand, if we focus on the beginning of the flights, during ascent, we see the clear effect of hysteresis that we initially attributed to ascent through thick cirrus clouds. However, a fortuitous test for the vacuum integrity of the inlet early in the Costa Rica mission resulted in a significant improvement in hysteresis and provided a representative protocol for drying out the instrument duct between flights. We illustrate this in Figure 12, where we compare flights on 20010807 and 20010809. The significant improvement on the 20010809 flight is attributed to the instrument pump-out between flights. This protocol was followed during the remainder of the Costa Rica mission as well as throughout the CRYSTAL mission with comparable success. Results from the remainder of the flights in Costa Rica as well as those during CRYSTAL FACE confirm that this laboratory protocol minimizes, but does not totally remove hysteresis during ascent.

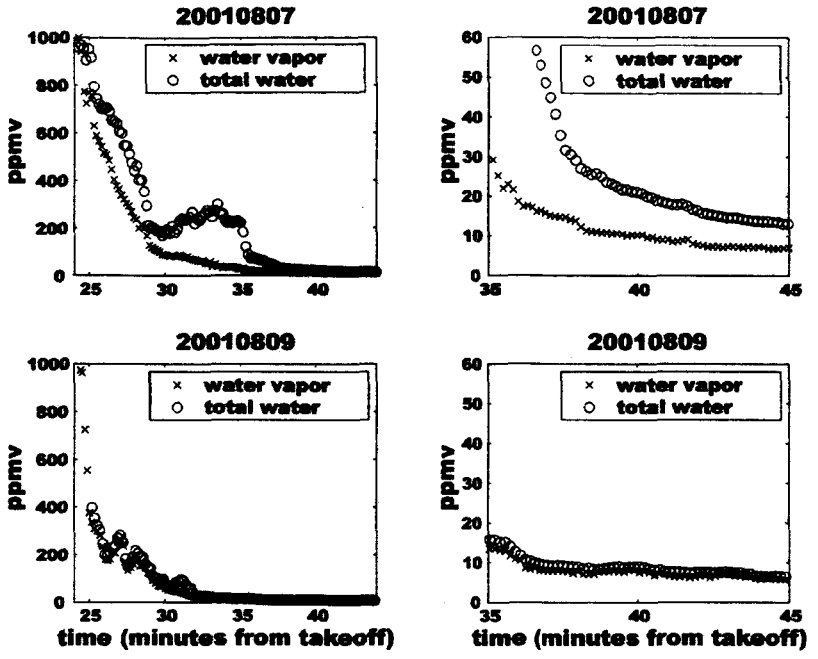

Figure 12. Measurements of water vapor and total water during ascent for two flights from San Jose, Costa Rica. The right-hand panels allow an intercomparison of the relative degree of hysteresis for the two flights, showing the marked improvement for the August 9 flight.

As further evidence of validation in clear air we turn to a flight during CF and present simultaneous measurements from both Harvard water instruments as well as the JPL tunable diode laser hygrometer [May, 1998]. This particular example provides a stringent test of the total water instrument, illustrating not only the agreement with the water vapor measurements, but also the absence of meaningful hysteresis.

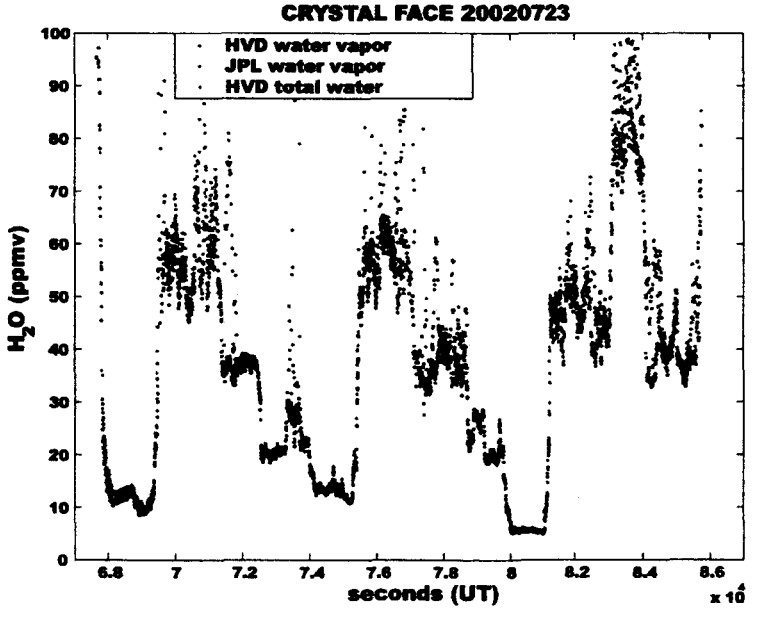

Figure 13. Comparison of water vapor instruments for the July 23, 2002 flight during CRYSTAL FACE showing agreement for the three instruments in clear air and the presence of clouds during positive excursions by total water.

Intercomparison with Other Total Water Instruments during CF

The opportunity was provided during CRYSTAL FACE to intercompare with two other total water instruments. One instrument, ALIAS, was modified to measure total water for the first time

using an isokinetic inlet and detection by multipass infrared absorption. [Webster et al., 1994]. The other, the University of Colorado (CU) total water instrument, measured total water vapor using a sensitivity enhancing anisokinetic inlet with single pass tunable diode laser infrared absorption for detection. We must emphasize that this intercomparison is not meant as a tool for critically evaluating the ultimate capabilities of either the CU or ALIAS instrument, as both were flying for the first time aboard the WB-57, and exhibit data quality problems that prevent meaningful data intercomparisons similar to that illustrated in Figure 13. As we will illustrate, understanding instrument sensitivities to cloud ice water content for these intercomparisons benefits from, if not requires, understanding their relative sensitivity to water vapor in clear air.

In Figure 14 we show an intercomparison of the three instruments for three flights in which all three worked successfully. We plot in each panel Harvard total water *versus* ALIAS total water, in clear air and cloudy air respectively, as well as Harvard ice water content *versus* CU ice water content. We compare the Harvard and ALIAS instrument measurements in clear air to determine the relative sensitivity of each instrument to water vapor. While in principle this factor should be one, reality is that it needs validation. The slope of the line serves as a reference or baseline for the intercomparison of the data in clouds. Based on a linear least squares fit to the data for flights on July 7, 9, and 11 flights that are reasonably self-consistent, we first determine that in clear air the two instruments agree, on average, remarkably and fortuitously well, with ALIAS/HVD = 1.01 ± 0.19. We say this because detailed studies of the data show that there are systematic differences in the instruments that just happen to cancel when the data is compared as in Figure 9. Nevertheless, when utilizing the "measured" sensitivity ratio, we then calculate that the ALIAS instrument is about 1.35 ± 0.21 more sensitive to particles. The uncertainties are 1-sigma and the uncertainty in the particle sensitivity ratio includes the statistical uncertainty in the clear air measurement sensitivity ratio. Unfortunately, the sensitivity of the CU instrument relative to our instrument in clear air cannot be validated by flight data. Because this single pass instrument utilizes for detection a well-studied water vapor infrared absorption feature, identical to the one used by May et al. [1998] in a hygrometer that has previously shown agreement with our water vapor instrument to ± 5%, we assume that in clear air the relative sensitivity of the Harvard and Colorado instruments is 1.0 ± 0.1. Then, using the data from the same three flights as before, we calculate that sensitivity to particles of the Colorado instrument is 0.73 ± 0.11 that of the Harvard. The most significant caveats to these conclusions are that these scatter plots do not reveal details that might help elucidate the discrepancies in measured water vapor and total water. For the comparison with the ALIAS instrument, determination of the relative sensitivity of the two instruments to water vapor is severely limited by hysteresis effects in ALIAS that are most prominent in the beginning of each flight and in dry air. Hysteresis is worse in the CU instrument, at least in part because of the slower flow rates used. We can only conclude that these data intercomparisons do not suggest any large systematic error in our ice water measurements, either from sampling effects or incomplete particle evaporation. While it cannot be ignored that all three instruments could leave some fraction of the cloud ice unevaporated, resulting in correlated errors that would remain hidden from these intercomparisons, this is less likely to be the case for the CU instrument that enhances particle sensitivity with anisokinetic flow.

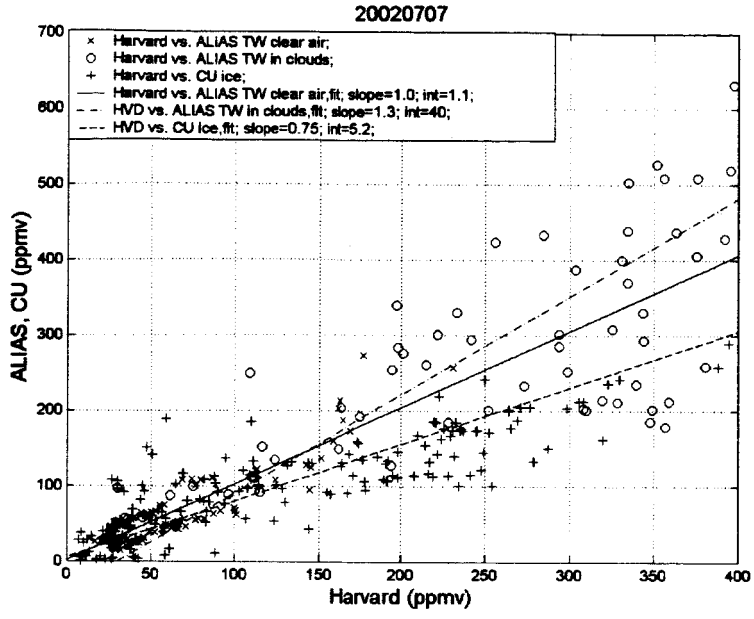
20020707
Harvard vs. ALIAS TW clear air;
Harvard vs. ALIAS TW in clouds;
Harvard vs. CU ice;
Harvard vs. ALIAS TW clear air,fit; slope=1.0; int=1.1;
HVD vs. ALIAS TW in clouds,fit; slope=1.3; int=40;
HVD vs. CU ice,fit; slope=0.75; int=5.2;
ALIAS, CU (ppmv)
Harvard (ppmv)
0
100
200
300
400
500
600
700
0
50
100
150
200
250
300
350
400

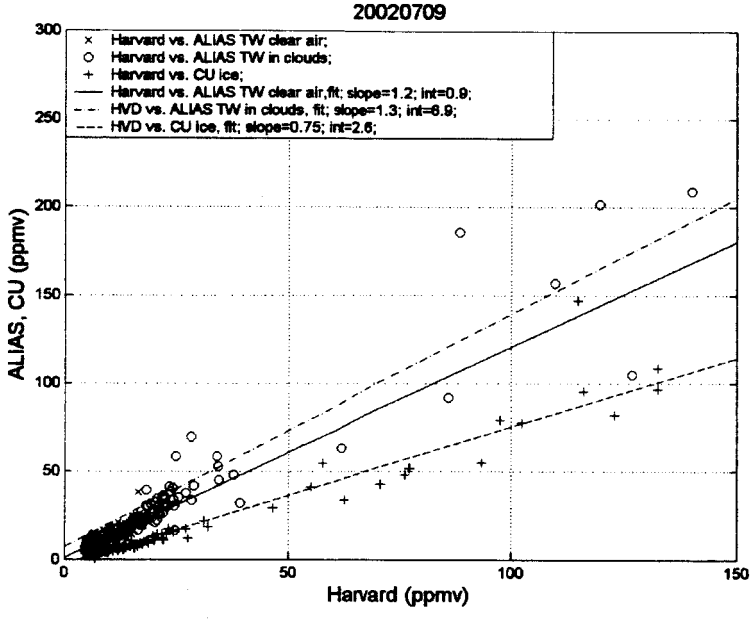
20020709
Harvard vs. ALIAS TW clear air;
Harvard vs. ALIAS TW in clouds;
Harvard vs. CU ice;
Harvard vs. ALIAS TW clear air,fit; slope=1.2; int=0.9;
HVD vs. ALIAS TW in clouds, fit; slope=1.3; int=6.9;
HVD vs. CU ice, fit; slope=0.75; int=2.6;
ALIAS, CU (ppmv)
Harvard (ppmv)
0
50
100
150
200
250
300
0
50
100
150

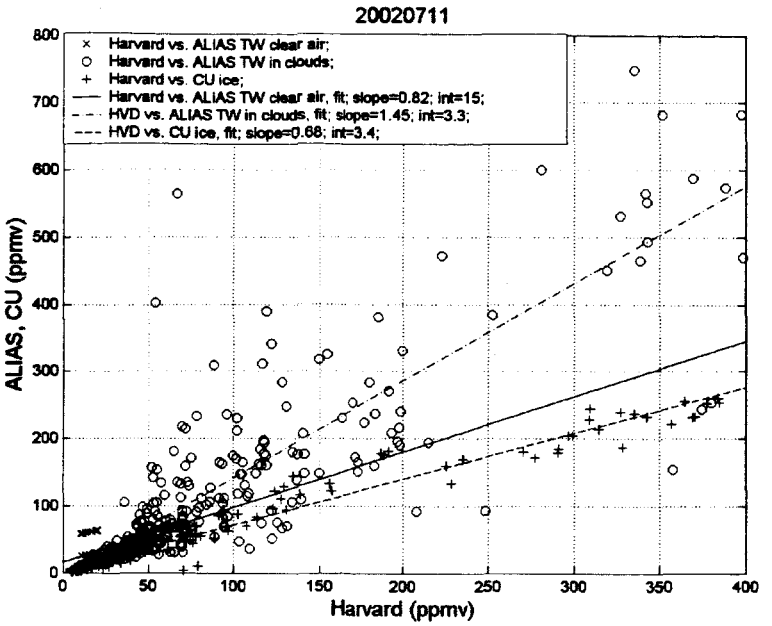

Figure 14. Plots of ALIAS and CU total water (y-axis) *versus* Harvard total water (x-axis). For the ALIAS intercomparisons the clear air and in-cloud data are plotted separately. The CU instrument only reports data in clouds. Included as well are linear least square fits to each data set. The three panels show data for the flights of July 7th, 9th, and 11th, 2002 respectively.

Instrument Accuracy

The total water instrument described here was specifically designed to enable accurate measurement of the ice water content of thin or subvisible cirrus near the tropical and subtropical tropopause. Our goal is to evaluate and quantify uncertainties in the ice water content measurement. While the instrument can and often does measure water vapor accurately, this measurement primarily serves to validate instrument operation, so observed hysteresis in the water vapor measurement does not directly add to the uncertainty in the total water measurement. On the other hand, hysteresis in the total water measurement in clouds of course does.

To quantify uncertainties in the total water instrument we define efficiency factors corresponding to the function of the four instrument subsystems described above:

1. Inlet particle density/ambient particle density;
2. Particle mass evaporated/duct particle mass;
3. Total water at the detection axis/total water entering the duct;
4. Actual sensitivity/sensitivity from calibration.

The total instrument uncertainty results from combining uncertainties in those efficiency factors. To determine uncertainty in the ice water content measurement requires including the uncertainty in the simultaneous water vapor measurement as well. We will show that this instrument pair provides cloud ice water measurements with an accuracy ranging from 9–17% depending on particle size distributions.

We start by noting that the minimum uncertainty, corresponding to number four above, is ±7%, based solely on the combined uncertainties in the detection axis sensitivities for the two water instruments, as has been established by the long history of water vapor measurements. We next consider the additional error from number three, which in essence results from hysteresis in the duct. This error as it impacts ice water measurements can be estimated using the hysteresis

observed after cloud transits on July 16, 2002, and illustrated in Figure 11b. We estimate from these data that at most 2% of the total water in clouds sticks to duct walls in the form of liquid droplets and then evaporates after the cloud transit. While it might be expected that this is a systematic error, lowering the ice water content measurement, this will depend on the specific cloud transit signature and could be positive when the total water signal is decreasing as the airplane is leaving the densest part of the cloud. We will therefore treat is as a random error. There is also the possibility that hysteresis will impact the determination of ice water content in thin cirrus, when measurements in clear air just before and after the cloud show evidence of hysteresis. While this can be accounted for by normalizing the clear air signal to that of the water vapor instrument, it does require an assumption that the degree of hysteresis changes smoothly through the cloud transect. While this cannot be strictly verified, it is only a concern when probing thin cirrus, where about 0.5 ppmv must be added to the overall uncertainty.

It is obvious from panel 1 in Figure 11 that at the transition between clear and cloudy air, the accuracy and precision in the cloud ice water becomes S/N limited. Typically, the precision in the measurement of water vapor and total water is 0.5 ppmv, but there are also instances when the total water instrument exhibits a small amount of hysteresis. This can be especially important when water vapor is low and ambient air temperature is low and decreases even further. We hypothesize that under these conditions the inlet takes up a little water, thereby measuring low. This manifested itself in Costa Rica, with total water measuring lower than water vapor under circumstances that coincided with a drop in ambient temperature. Because this could be an important issue, we explore it further with two examples from two flights during the CF mission. In figure 15 panel (a) and (e) we plot simultaneous measurements of water vapor from the two Harvard instruments and the JPL instrument. Panels (b) and (f) provide ambient temperature, panels (c) and (g) plot the fractional difference between pairs of instruments. In panels (d) and (h) the roots pump rpm is plotted. The relative drop in total water signal, corresponding to about 0.5 ppmv or 10% observed water vapor, coincides in each case with the change in pump rpm. The resulting slowdown in velocity apparently leads to some surface water adsorption, most likely on the cold inlet. What these plots reveal is that because of the design requirements of a total water instrument, both mechanically and operationally where isokinetic flow is needed, the risk of incurring systematic errors from surface effects must be carefully explored. While the errors shown here are small and only occur when ambient water vapor is low, this is the regime where the ice water content of thin cirrus must be measured with critical care. A 10% error in the water vapor measurement will propagate into an error in ice water content proportional to the ratio of water vapor to total water. Analysis of the full data set suggests that in the tropopause region where thin cirrus clouds are sampled the surface only acts to adsorb and not desorb. Accordingly, without having the water vapor instrument as a check on the total water instrument, this 10% error could cause the ice water measurement in this region to be low by 10*(wv/tw)%.

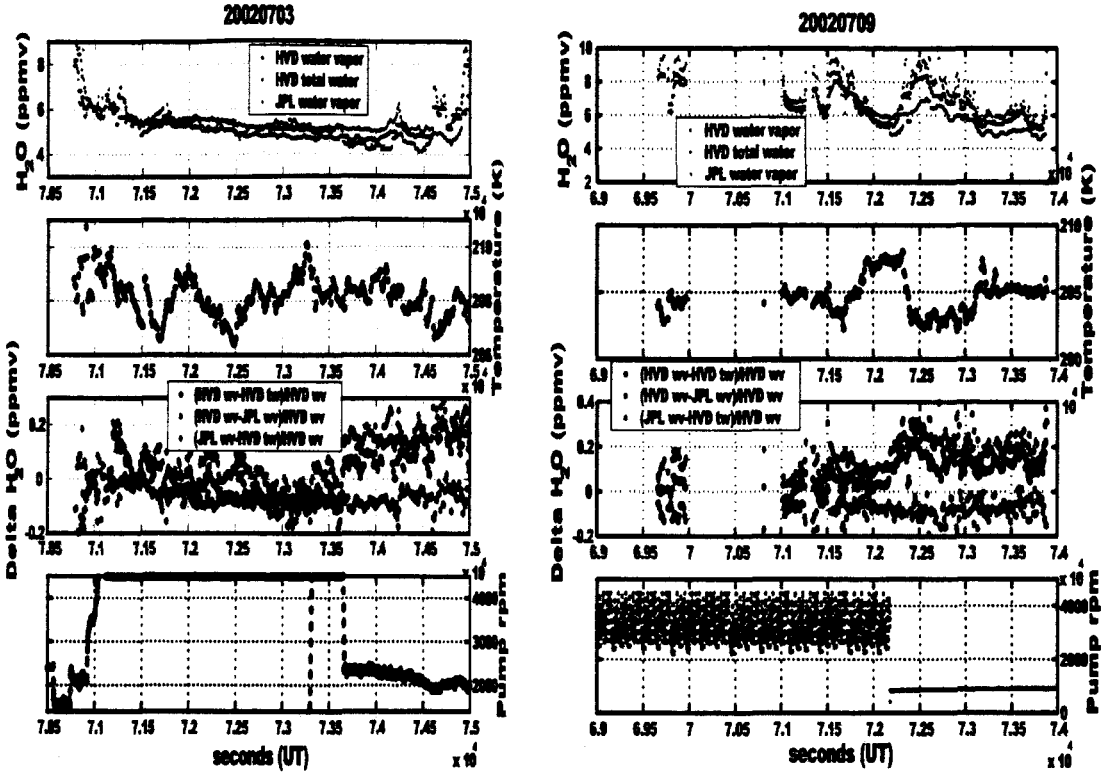

Figure 15. Intercomparison of total water measurements in cloud-free air with the Harvard and JPL water vapor instruments for flights on July 3, and July 9, 2002. The bottom panels plot pump rpm, showing the transition from high to low speed on the 3rd, and from high speed to off on the 9th. In each case the total water instrument measures low starting from the time that the duct velocity slows down.

Comparing the data from the two flights, we see here that there is a slight dependence on pump speed/flow velocity. This manifests itself in the relatively unusual relationship between pump speed and signal, with water increasing as pump speed increases. Because with water vapor measurements conventional wisdom regarding systematic errors is that when in doubt go with the lesser amount of water. This would imply that the instrument has a systematic error causing it to measure more accurately at slower flow speeds, behavior that is inconsistent with our broad experience base in measuring water vapor. The intercomparison with the JPL hygrometer provides evidence consistent with our interpretation of the instruments measuring low, under certain conditions. A misinterpretation of this would incorrectly place suspicion on the accuracy of the water vapor instrument at low water vapor mixing ratios.

To illustrate instrument capability, we plot in Figure 16 as an example of the detection of thin cirrus near the tropical tropopause, water vapor, total water, relative humidity, and ozone as a function of altitude. In this figure we show the more than adequate signal-to-noise the instrument exhibits in precisely (and accurately) measuring the ice water content of thin cirrus. While discussion of the full implications of these data is beyond the scope of this paper, we note that in the cloud, the minimum water vapor observed is just under 6 ppmv, but that the minimum saturation mixing ratio is 4 ppmv at the top of the cloud. On average, 2 ppmv of water remains in the vapor phase that would be in the solid phase if relative humidity in the cloud decreased to 1.

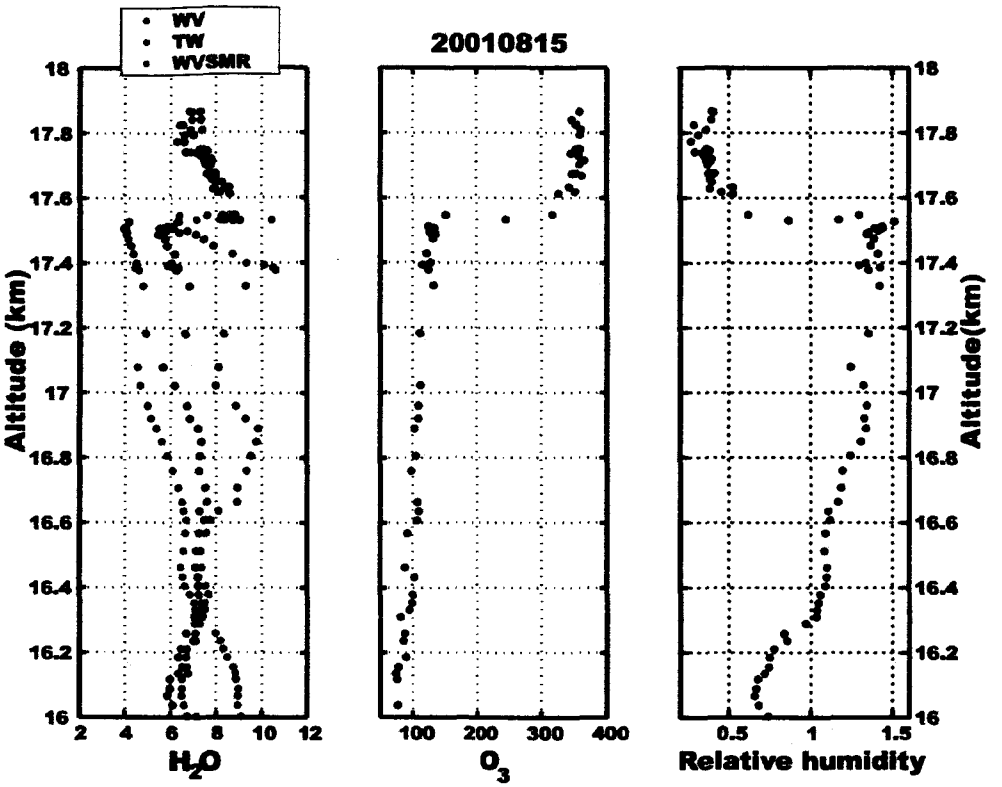

Figure 16. Plot showing measurements of the thin cirrus cloud at the tropopause on August 15, 2001. The sharp tropopause is clearly shown by both the ozone and relative humidity profiles.

Thus, in this cloud, the dehydration potential of the air mass containing this cloud is not realized and any calculation that assumes dehydration to the saturation mixing ratio based on the measured temperature (e.g. Vomel et al., 2002) would be invalid (Dessler and Weinstock, 2002). Above the temperature minimum at the top of the cloud, at about 17.6 km, water vapor rises sharply from its minimum of 6 ppmv to above 8 ppmv, and then gradually decreases with increasing altitude. The ozone profile in panel 2 exhibits further evidence of the local tropopause as a barrier to mixing. The plot of relative humidity in panel 3 illustrates the effect of the sharp increase in temperature at the tropopause.

The next source of error, corresponding to number 2 above, results from incomplete particle evaporation. Based on simple calculations for evaporation of droplets, we have established that particles with diameters up to 100μm are completely evaporated. It is reasonable to be concerned that fractions of larger particles remain unevaporated, with that fraction proportional to the initial particle diameter. Parameterizations of effective ice particle density as a function of particle diameter [Heymsfeld et al., 2003], and comparisons with total water measurements from the MASP instrument, suggest the possibility that Harvard ice water measurements are low when large particles are present. As discussed earlier, scattering data at the detection axis in general scales with measured total water and is consistent with incomplete evaporation. One would expect that this scattering signal would scale with the difference between Harvard and MASP ice water content. However, there are examples during cloud events where there is significant scattering and the two total water measurements agree very well, and other cases where there is significant disagreement but only a small scattering signal. Furthermore, because ice water

content derived from an instrument that measures particle scattering, one necessarily must assume an effective ice density that is likely to have a dependence on particle size. Nevertheless, the presence of a scattering signal does suggest that, at least for ice water content above about 500 ppmv, incomplete evaporation provides a source of uncertainty that is virtually impossible to quantify. We will not include this in the quoted error bars for the instrument and will address needed instrument updates later in the manuscript.

We next address item 1, maintenance of ambient particle density in the duct. Not only the design of the inlet, but also the position of the inlet relative to the WB-57 fuselage, was predicated on measuring the water vapor content for particles up to 50 microns in diameter by satisfying this criterion within 10%. As previously discussed, flow perturbations by the fuselage at the inlet partially cancel the impact on particle density from deviations from isokinetic conditions. Nevertheless, neither of these contributions to measurement uncertainty has been verified, so we estimate an additional 15% uncertainty for particles larger than 20μm caused by these flow perturbations, leading to a total uncertainty of 17% in the ice water content of thick cirrus. For thin cirrus or contrail encounters, we reduce this to 5%, thus leading to a total uncertainty of 9%.

Instrument improvements

We have provided detailed evidence for the quoted accuracy and precision of the total water vapor instrument. Additionally, we have illustrated how agreement between the total water and water vapor instruments in spite of their operational differences further support that accuracy for the water vapor instrument. Based on the information provided here, there are two specific areas that can be improved. First, measurement of ambient pressure and velocity at the inlet will remove the uncertainty in those number based on model calculations of the flow around the aircraft. Secondly, to help resolve the question of low water vapor measurements in the lower stratosphere, we plan to modify the inlet to not only to enable sufficient heating, but also to Teflon coat it, and the instrument duct as well. Concerns regarding temperatures insufficient to totally evaporate large particles will be resolved by combining additional heat with a high conductance screen with 50 μm diameter holes to break up large ice particles.

Conclusions

In this paper we have demonstrated the performance of a total water instrument that when combined with simultaneous water vapor measurements from the Harvard photofragment fluorescence hygrometer provides ice water mixing ratios with an accuracy of 9% in thin cirrus and 17% in thicker cirrus when particle diameters are 20 μm or larger. Examples of total water measurements in cirrus clouds ranging from subvisible cirrus in the tropics to dense cirrus in the subtropics are given. Accurate measurement of water vapor in the atmosphere continues to be a challenge even though instrumental techniques exist that are amenable to laboratory calibration methods and successful in-flight intercomparisons have been performed. Total water measurements are similarly limited in accuracy with the further uncertainty derived from having to maintain the ice particle density in the air sample as it transitions from ambient conditions to the instrument. While we have designed the inlet to limit the perturbation to that density, further validation of these measurements is desirable. We first plan to make the aforementioned improvements to the instrument. We are also in the process of making upgrades in the water vapor instrument in order to achieve "benchmark" status. Nevertheless, even if these modifications are successful, we look to the history of water vapor intercomparisons as a guide to what might be necessary to promote confidence in the total water measurements. On the one

hand, the intercomparisons with two other total water instruments during CF provide some confidence that our cloud ice water content measurements are good to at least 30%. However, because hysteresis has prevented both instruments from measuring water vapor in clear air with an accuracy that can substantiate its assumed sensitivity, the confidence one can draw from the aforementioned intercomparisons as plotted in figure 10 is limited. We expect that significant improvement in one or both of the other total water instruments will take place. Fortunately, integration onto the WB-57 of the CVI cloud ice water content instrument is underway in preparation for a mission that includes in its list of objectives total water intercomparisons.

References

Boering, K. A., B. C. Daube, S. C. Wofsy, M. Loewenstein, J. R. Podolske, and E. R. Keim, Tracer-tracer relationships and lower stratospheric dynamics: CO_2 and N_2O correlations during SPADE, *Geophys. Res. Lett.* **21**, 2567–70, 1994.

Dessler, A. E. and E. M. Weinstock, Comment on "Balloon-borne observations of water vapor and ozone in the tropical upper troposphere and lower stratosphere" by H. Vomel et al., J. Geophys. Res., 108(D4), doi: 10.1029/2002JD002811, 2003.

Engblom, W. A. and M. N. Ross, Numerical model of airflow induced particle enhancement for instruments carried by the F aircraft, Aerospace Report NO. ATR-2004(5084)-1, 2003.

Heymsfeld, A. J., A. Bansemer, C. Schmitt, C. Twohy, and M. R. Poellot, Effective ice particle densities derived from aircraft data, *J. Atmos. Sci.*, submitted.

Heymsfeld, A. J., C. G. Schmitt, A. Bansemer, D. Baumgardner, E. M. Weinstock, and J. Smith, Effective ice particle densities for cold anvil cirrus, submitted.

Hinds, William C. (1999), *Aerosol Technology: Properties, Behaviour, and Measurement of Airborne Particles*, second edition, John Wiley and Sons, NY.

Hintsa, E. J., E. M. Weinstock, J. G. Anderson, and R. D. May, On the accuracy of in situ water vapor measurements in the troposphere and lower stratosphere with the Harvard Lyman-α hygrometer, *J. Geophys. Res.* **104**, 8183–9, 1999.

Kelly K. K., M. H. Proffitt, K. R. Chan, M. Loewenstein, J. R. Podolske, S. E. Strahan, J. C. Wilson, and D. Kley, Water vapor and cloud water measurements over Darwin during the STEP 1987 tropical mission, *J. Geophys. Res.* **98**, 8713–24,1993

King, W. D., Airflow and particle trajectories around aircraft fuselages, I. Theory, *J. Atmos. Ocean. Technol.* **1**, 5–13,1984.

King, W. D., D. E. Turvey, D. Williams, and J. Llewellyn, Airflow and particle trajectories around aircraft fuselages, II. Measurements, *J. Atmos. Ocean. Technol.* ***1***, 14–21,1984.

King, W. D., Airflow and particle trajectories around aircraft fuselages, III. Extensions to particles of arbitrary shape, *J. Atmos. Ocean. Technol.* **2**, 539–47,1985.

Kley, D., E. J. Stone, W. R. Henderson, J. W. Drummond, W. J. Harrop, A. L. Schmeltekopf, T. L. Thompson and R. H. Winkler, In situ measurements of the mixing ratio of water vapor in the stratosphere, *J. Atmos. Sci.* **36**, 2513–24, 1979.

Liou, K.N., P. Yang, Y. Takano, K. Sassen, T.P. Charlock, and W.P. Arnott, 1998: On the radiative properties of contrail cirrus. *Geophys. Res. Lett.* **25**, 1161–4.

May, R. D., Open-path, near-infrared tunable diode laser spectrometer for atmospheric measurements of H_2O, *J. Geophys. Res.* **103**, 19161–72, 1998.

McFarquhar et al., Thin and subvisible tropopause tropical cirrus: observations and radiative impacts, *J. Atmos. Sci.* **57**, 1841–53, 2000.

Murphy, D. M., and M. E. Schein, Wind tunnel tests of a shrouded aircraft inlet, *Aerosol Sci. Technol.* **28**, 33–8, 1998.

Pfister, Leonard et al., Aircraft observations of thin cirrus clouds near the tropical tropopause, *J. Geophys. Res.* **106**, 9765–86, 2001.

Pruppacher H. R. and J. D. Klett (1978), *Microphysics of Clouds and Precipitation*, Second Edition, Kluwer Academic Publishers, Norwell, MA.

Rader, D. J., and V. A. Marple, A study of the effects of anisokinetic sampling, *Aer. Sci. Tech.* **9**, 283–99, 1988.

Rasmussen, R. M., V. Levizzani and H. Pruppacher, A wind tunnel and theoretical study of the melting behaviour of atmospheric ice particles II: A theoretical study for frozen drops of radius < 500 μm, *J. Atmos. Sci.* **41**, 374–80, 1984.

Schiller, C. et al., Ice particle formation and sedimentation in the tropopause region: A case study based on in situ measurements of total water during POLSTAR 1997, *Geophys. Res. Lett.* **26**, 2219–22, 1999.

Soderman P. T., N. L. Hazen, W. H. Brune, Aerodynamic design of gas and aerosol samplers for aircraft, NASA Technical Memorandum 103854, 1-14, September, 1991.

Kley, D., J. M. Russell III, C. Phillips (Eds.) *SPARC Assessment of Upper Tropospheric and Stratospheric Water Vapour*, rep. 113, World Clim. Res. Programme (WCRP), Geneva, Switzerland, December 2000.

Stackhouse, P. W. Jr., and G. L. Stephens, A Theoretical and observational study of the radiative properties of cirrus: results from FIRE 1986, *J. Atmos. Sci.* **48**, 2044–59, 1991.

SPARC Assessment of Upper Tropospheric and Stratospheric Water Vapour, WCCRP N° 113, WMO/TD-N° 1043 (December 2000)

Stephens, G. L. et al., THE CLOUDSAT mission and the A-TRAIN, a new dimension of space-based observations of clouds and observations of clouds and precipitation, *BAMS*, 1771–90, 2002.

Twohy, C. H., A. J. Schanot, and W. A. Cooper, *J. Atmos. Oceanic Technol.* **14**, 197–202, 1997.

Vomel, H. et al., Balloon-borne observations of water vapor and ozone in the tropical upper troposphere and lower stratosphere, J. Geophys. Res., 108, doi: 10.1029/2002JD002984, 2003.

Webster, C. R., R. D. May, C. A. Trimble, R. G. Trave, and J. Kendall, Aircraft (ER2) laser infrared absorption spectrometer (ALIAS) for in-situ stratospheric measurements of HCl, N_2O, CH_4, NO_2, and HNO_3, *Applied Optics* **33**, 454–72, 1994.

Webster, C. R. and A. J. Heymsfeld, Water isotope ratios D/H, $^{18}O/^{16}O$, $^{17}O/^{16}O$ in and out of clouds map dehydration pathways, *Science* **302**, 1742–5, 2003.

Weinstock E. M., J. J. Schwab, J. B. Nee, M. J. Schwab, and J. G. Anderson, A cryogenically cooled photofragment fluorescence instrument for measuring stratospheric water vapor, *Rev. Sci. Instrum.* **61**, 1413–32, 1990.

Weinstock, E. M., *et al.*, "New fast response photofragment fluorescence hygrometer for use on the NASA ER-2 and the Perseus remotely piloted aircraft," *Rev. Sci. Instrum.* 65, 3544–54, 1994.

Zöger, M., et al., Fast in situ stratospheric hygrometers: A new family of balloon-borne and airborne Lyman-α photofragment fluorescence hygrometers, *J. Geophys. Res.* **104**, 1807–16, 1999.